**NEURAL REGENERATION RESEARCH**
December 2014, Volume 9, Issue 24
www.nrronline.org

# Hyperbaric oxygen therapy improves local microenvironment after spinal cord injury

**Yang Wang[1], Shuquan Zhang[2], Min Luo[1], Yajun Li[3]**

1 Department of Orthopedics, China-Japan Union Hospital, Jilin University, Changchun, Jilin Province, China
2 Department of Orthopedics, Nankai Hospital, Tianjin, China
3 School of Mathematics, Jilin University, Changchun, Jilin Province, China

***Corresponding author:***
*Yajun Li, School of Mathematics, Jilin University, Changchun 130028, Jilin Province, China, yanyao523@163.com.*

***doi:****10.4103/1673-5374.147951*
***http:****//www.nrronline.org/*

***Accepted:*** *2014-11-20*

## Abstract

Clinical studies have shown that hyperbaric oxygen therapy improves motor function in patients with spinal cord injury. In the present study, we explored the mechanisms associated with the recovery of neurological function after hyperbaric oxygen therapy in a rat model of spinal cord injury. We established an acute spinal cord injury model using a modification of the free-falling object method, and treated the animals with oxygen at 0.2 MPa for 45 minutes, 4 hours after injury. The treatment was administered four times per day, for 3 days. Compared with model rats that did not receive the treatment, rats exposed to hyperbaric oxygen had fewer apoptotic cells in spinal cord tissue, lower expression levels of aquaporin 4/9 mRNA and protein, and more NF-200 positive nerve fibers. Furthermore, they had smaller spinal cord cavities, rapid recovery of somatosensory and motor evoked potentials, and notably better recovery of hindlimb motor function than model rats. Our findings indicate that hyperbaric oxygen therapy reduces apoptosis, downregulates aquaporin 4/9 mRNA and protein expression in injured spinal cord tissue, improves the local microenvironment for nerve regeneration, and protects and repairs the spinal cord after injury.

***Key Words:*** *nerve regeneration; spinal cord injury; hyperbaric oxygen; motor function; rats; microenvironment; aquaporin 4; aquaporin 9; neural regeneration*

***Funding:*** *This study was financially supported by grants from the Science and Technology Development Project of Jilin Province in China, No. 20110492.*

*Wang Y, Zhang SQ, Luo M, Li YJ. Hyperbaric oxygen therapy improves local microenvironment after spinal cord injury. Neural Regen Res. 2014;9(24):2182-2188.*

## Introduction

Restoration of motor function is the primary goal of clinical rehabilitation after spinal cord injury (Pallini et al., 2005). Methods by which to promote nerve regeneration and recover neurological function have been widely investigated in the clinic and in medical research. At present, clinical treatment of spinal cord injury includes the use of neurotrophic factors and physical rehabilitation, which contribute to the repair of necrotic tissue, attenuate spinal cord ischemia and hypoxia, and promote the recovery of neuronal function (Pallini et al., 2005; Pearse et al., 2007; Chuang, 2011; Ariake et al., 2012). However, such treatments remain unsatisfactory because of their high costs, adverse effects, and frequent complications.

Hyperbaric oxygen therapy is a promising new strategy in the process of rehabilitation after brain or spinal cord injuries (Fenton et al., 1993). The treatment involves breathing pure oxygen in a sealed chamber pressurized to 1–3 times normal atmospheric pressure. It promotes the proliferation and differentiation of endogenous stem cells, increases arterial partial pressure of oxygen, elevates blood oxygen content in the central nervous system, promotes aerobic metabolism in the central nervous system, and ameliorates secondary damage in spinal cord injury (Mukai et al., 2002; Chuang, 2011; Ding, 2012). In addition, hyperbaric oxygen therapy reduces malondialdehyde and calcium ion content, inhibits lipid peroxidation, enhances the antioxidant capacity of the cell membrane, reduces intracellular calcium ion concentration, protects nerve cells and promotes nerve regeneration (Liu et al., 2004; Guo and Dong, 2009; Kunke et al., 2009; Tong et al., 2010; Chang et al., 2011; Chuang, 2011; Gomez-Iturriaga et al., 2011; Ding, 2012; Guo et al., 2013; Jiao et al., 2013; Xiong et al., 2014; Yu et al., 2014).

A major obstacle in the clinical treatment of spinal cord injury is the inability of damaged axons to regenerate. This may be due to the release of inhibitory factors that are not conducive to neurite growth in the spinal cord microenvironment. Increasing evidence from clinical studies has shown that hyperbaric oxygen therapy significantly improves the microenvironment around the injured spinal cord and reduces secondary nerve damage (Meletis et al., 2008). The aim of the present study was to explore the effects of hyperbaric oxygen therapy on the microenvironment of the injured spinal cord, and its role in nerve regeneration and electrophysiological function.

## Materials and Methods

### Animals

Sixty-seven clean-grade adult female Sprague-Dawley rats, aged 3 months and weighing 250–290 g, were provided by the Laboratory Animal Center of Tianjin Medical University of China (license No. SCXK (Jin) 20070001). Rats were housed in temperature-controlled (25°C) and humidity-controlled (45%) conditions, under natural light. The study was approved by the Experimental Animal Ethics Committee of Jilin University, China.

### Establishing rat models of spinal cord injury

Forty-seven rats were anesthetized by intraperitoneal injection of 10% chloral hydrate (350 mg/kg) and fixed in the prone position on an operating table. A midline skin incision was made to expose the spinous processes and lamina at $T_{7–10}$. Spinous processes $T_{8–9}$ and part of the lamina were stripped, but the dura mater remained intact. A weight of 10 g was dropped onto the dura mater and spinal cord from a height of 50 mm. The spinal cord injury model was considered successful when the hind legs and tail twitched spastically several times until flaccid paralysis occurred (Young, 2002). The wound was rinsed with hydrogen peroxide and sutured. Manual bladder expression was performed in all rats 2–3 times daily until the micturition reflex was restored. Four rats died during surgery and three rats were excluded owing to modeling failure. The remaining 40 rats were randomly and equally divided into a model group and a hyperbaric oxygen therapy group. Another 20 rats served as the sham group, in which the spinal cord tissue was exposed but no weight was dropped.

### Hyperbaric oxygen therapy

In the hyperbaric oxygen therapy group, rats were placed in a hyperbaric oxygen chamber (Shanghai 701; Yang Garden Hyperbaric Oxygen Chamber Co., Ltd., Shanghai, China) for 45 minutes, 4 hours after injury. The chamber was washed with pure oxygen for 15 minutes and pressurized to 0.2 MPa at a rate of 0.01 MPa/min. The pressure was stabilized for 30 minutes, and pure oxygen was intermittently added to the chamber to maintain a concentration over 96.5%. Pressure in the chamber was then reduced to atmospheric and rats were returned to their home cages. Rats in the hyperbaric oxygen group underwent this procedure four times per day for 3 consecutive days.

### Motor function assessment

Eight rats in each group were selected for motor function testing before and 1, 3, 7, 14, 21 and 28 days after modeling. According to the Basso-Beattie-Bresnahan (BBB) rating system (Finch et al., 1999; Papastefanaki et al., 2007), hindlimb motor function was rated on a 21-point scale, with scores ranging from 0 (indicating total paralysis) to 21 (indicating normal locomotion). In the inclined plane test, rats were placed on a smooth platform, with the body parallel to the axis of the plane. The plane was tilted in 5° increments and the greatest angle at which rats could maintain a stable position for 5 seconds was recorded (Pallini et al., 2005; Albin and Mink, 2006). Animals were also assessed using modified Tarlov scores, as follows: 0, no hindlimb activity, unable to bear weight; 1, visible hindlimb activity but unable to bear weight; 2, frequent or powerful hindlimb activity but unable to bear weight; 3, hindlimb can bear weight and animal can take 1–2 steps; 4, animal can walk, with mild impairment; 5, normal walking (Papastefanaki et al., 2007; Pearse et al., 2007).

### TUNEL assay for detection of apoptosis in the injured spinal cord

Five rats in each group were anesthetized with chloral hydrate 72 hours after spinal cord injury, and perfused with 4% paraformaldehyde solution *via* the left ventricle and aorta. A 2 cm length of spinal cord was harvested from the injury site and postfixed in paraformaldehyde. The tissue was embedded in paraffin and 20 μm sections were cut. Sections were deparaffinized, antigen retrieval was performed with proteinase K at 37°C for 30 minutes, and the sections were rinsed with PBS (pH 7.4) three times for 5 minutes each time, before incubation with 20% fetal calf serum and 3% bovine serum albumin at 37°C for 15 minutes. The reaction was terminated with 5 μL TdT and 45 μL fluorescein-labeled oligodeoxynucleotide buffer (Roche, Penzberg, Germany) for 1 hour in a 37°C chamber. Endogenous peroxidase was blocked with 0.3% $H_2O_2$, and the sections were incubated with 20% goat serum, 3% bovine albumin serum and 1% blocking agent at 37°C for 15 minutes, before immunoreaction with POD (HRP conjugated anti-fluorescein antibody, 20 μL, 1:2) in a wet box at 37°C for 30 minutes. Staining was visualized with DAB-$H_2O_2$. The sections were counterstained with hematoxylin, dehydrated through an ethanol series, rendered transparent using xylene, and mounted. Between each step, the sections were rinsed with PBS (pH 7.4) three times, for 5 minutes each time. Apoptotic cells were counted under an optical microscope (Olympus, Tokyo, Japan) at 200× magnification.

### Reverse transcription PCR for measurement of aquaporin 9 (AQP9) and aquaporin 4 (AQP4) mRNA expression in the injured spinal cord

A further five rats in each group were selected and sacrificed under anesthesia 72 hours after spinal cord injury, and 50 mg spinal cord tissue was harvested. Total RNA was extracted using a TRIzol kit (TaKaRa Company, Dalian, Liaoning Province, China), according to the manufacturer's instructions. RNA content was determined with a UV spectrophotometer (Beijing CBIO Bioscience & Technologies Co., Ltd., Beijing, China). The mRNA was reversely transcribed into cDNA using the two-step reverse transcription PCR kit (TaKaRa Company) and the obtained cDNA was amplified by PCR using the following parameters: 95°C pre-degeneration for 5 minutes and 40 cycles of degeneration at 95°C for 30 seconds, annealing at 60°C for 30 seconds, and extension at 72°C for 30 seconds.

Primer sequences are as follows:

| Primer | Sequence | Product length (bp) |
|---|---|---|
| AQP9 | Upstream 5′-CCA GCT CCA TTC ATA TCC AC-3′<br>Downstream 5′-CTA ATG ACA ACA GGC TCC AG-3′ | 137 |
| AQP4 | Upstream 5′-CCA GCT GTG ATT CCA AAA CGG AC-3 ′<br>Downstream 5′-TCT AGT CAT ACT GAA GAC AAT ACC TC-3 ′ | 305 |
| β-Actin | Upstream 5′-CCA TCA TGA AGT GTG ACG TTG-3′<br>Downstream 5 ′-ACA GAG TAC TTG CGC TCA GGA-3′ | 175 |

The amplification product was electrophoresed at 120 V and 50 mA for 15–30 minutes, and the optical density was analyzed using a gel electrophoresis image analysis system (Shanghai Haishen Medical Electronic Instrument Co., Ltd., Shanghai, China). The AQP4/9 mRNA expression level was calculated as the integrated optical density ratio of AQP4/9 to β-actin.

**Western blot analysis of AQP9 and AQP4 expression in the injured spinal cord**

At 72 hours after spinal cord injury, five rats in each group were sacrificed under anesthesia and spinal cord tissue was harvested. Samples were centrifuged at 1,500 r/min for 30 minutes, and total protein concentration in the supernatant was determined. The samples were then electrophoresed in 5% stacking gel at 40 V for 1 hour and 10% separating gel at 60 V for 3.5 hours, and transferred onto a PVDF membrane at 14 V for 14 hours. The membrane was blocked at 37°C for 2 hours, rinsed three times in TBS for 10 minutes each time, and incubated with rabbit anti-AQP9/AQP4 polyclonal antibody (1:500; Sigma, St. Louis, MO, USA) and rabbit anti-β-actin polyclonal antibody (1:500; Sigma) at room temperature for 60 minutes. After three washes in TBST, samples were incubated with alkaline phosphatase-labeled goat anti-rabbit IgG (1:2,000; Sigma) at room temperature for 60 minutes, developed with DAB (Beijing CellChip Biotechnology Co., Ltd., Beijing, China), and analyzed using Quantity One imaging software (Bio-Rad, Hercules, CA, USA). The AQP4/9 protein expression level was calculated as the integrated optical density ratio of AQP4/9 to β-actin.

**Hematoxylin-eosin staining for pathological changes in the rat spinal cord**

Four weeks after spinal cord injury, five rats in each group were anesthetized with 10% chloral hydrate (350 mg/kg) and fixed in paraformaldehyde. The injured spinal cord tissue was harvested, dehydrated through an ethanol gradient, and cut into longitudinal sections at a thickness of 20 μm using a cryostat. The sections were stained with hematoxylin for 5 minutes, rinsed with tap water, differentiated in hydrochloric acid for 10 seconds, rinsed with tap water for 10 minutes, stained with eosin for 7 minutes, dehydrated through an ethanol gradient, rendered transparent with xylene, and mounted. The sections were observed under an optical microscope.

**NF-200 expression in the injured spinal cord as detected by immunohistochemistry**

Alternative sections from the tissue harvested for hematoxylin-eosin staining were used for immunohistochemistry. The frozen sections were warmed to room temperature for 30 minutes and blocked with fetal calf serum for 1 hour. After three PBS washes, sections were incubated with rabbit anti-NF-200 IgG polyclonal antibody (1:100; Chemicon, Santa Cruz, CA, USA) at 4°C overnight, and goat anti-rabbit IgG (1:100; Chemicon) at 37°C for 2 hours. Proteins were visualized with DAB (Beijing CellChip Biotechnology Co., Ltd.) for 5–10 minutes and the reaction was terminated using tap water, followed by ethanol gradient dehydration, xylene transparency, and mounting. Ten fields of view per section were randomly chosen for analysis at 200× magnification, and NF-200-positive nerve fibers were quantified with Image-Pro Plus 6.0 software (Media Cybernetics, Silver Spring, MD, USA).

**Assessment of neurological function in rat hindlimbs**

Four weeks after spinal cord injury, seven rats in each group were selected, somatosensory evoked potentials and motor evoked potentials were measured with a Keypoint 4 evoked potential device (Beijing Weidi Kangtai Medical Instrument Co., Ltd., Beijing, China). In brief, rats were anesthetized with an intraperitoneal injection of 10% chloral hydrate (350 mg/kg) and fixed in the horizontal plane. For somatosensory evoked potential measurements, stimulating electrodes were inserted in the gluteus maximus, recording electrodes were placed in the hindlimb cortical sensory areas (Paxinos and Watson, 2005) below the intersection between the coronal and sagittal sutures, and reference electrodes were positioned 0.5 cm posterior to the recording electrodes. Electrical stimulation parameters were as follows: direct current square wave, 5–15 mA intensity, 0.2 ms width, 3 Hz frequency, 50–60 superimposed pulses, until a slight twitch was observed in the hindlimb. The somatosensory evoked potential latency and amplitude were recorded (Block et al., 1993).

To calculate motor evoked potentials, the stimulating electrodes were placed in the motor cortex (2 mm anterior to the top coronal suture and 2 mm lateral to sagittal suture). Electrical stimulation parameters were as follows: 40 mA intensity, 0.1 ms width, 1 Hz frequency, 300–500 superimposed pulses, scanning sensitivity = 5 μV/D, scanning speed = 5 ms/D. The motor evoked potentials latency and amplitude were recorded (Albin and Mink, 2006).

**Statistical analysis**

Statistical analysis was performed by the second author using SPSS 17.0 software (SPSS, Chicago, IL, USA). Data were expressed as the mean ± SD, and repeated measures analysis

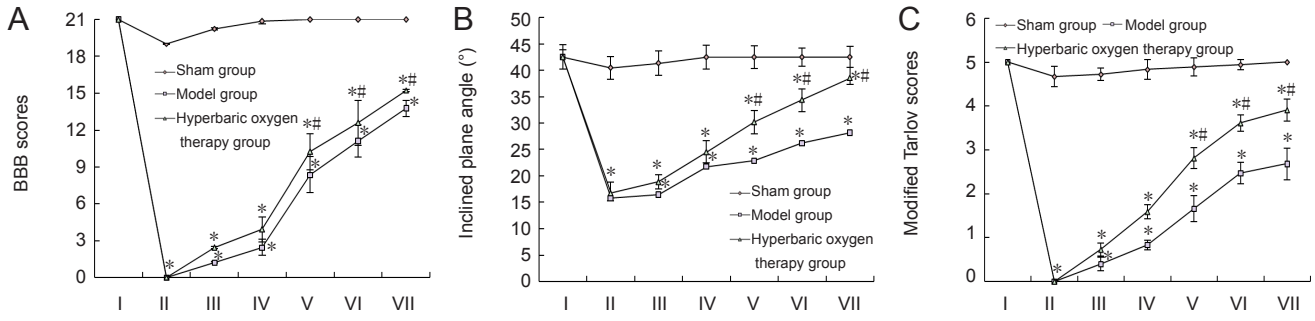


**Figure 1 Effect of hyperbaric oxygen therapy on motor function in rats with spinal cord injury.**
Rats exposed to hyperbaric oxygen had higher BBB scores (A), reached greater angles on the inclined plane test (B) and had higher modified Tarlov scores (C) than model rats, indicating better motor function. Data are expressed as the mean ± SD ($n = 8$ rats per group). *$P < 0.05$, *vs.* sham group; #$P < 0.05$, *vs.* model group (repeated measures analysis of variance and the Student-Newman-Keuls test). I: Before modeling; II–VII: 1 day, 3 days, 1, 2, 3, 4 weeks post-modeling; BBB: Basso-Beattie-Bresnahan scale.

of variance and the Student-Newman-Keuls test were performed. $P < 0.05$ was considered significant.

## Results

### Hyperbaric oxygen therapy improved hindlimb motor function in rats with spinal cord injury

Before spinal cord injury, BBB scores, inclined plane angle and modified Tarlov scores were not significantly different between the three groups. After spinal cord injury, all measures were significantly lower in the model and hyperbaric oxygen groups than in the sham group ($P < 0.05$), and 2–4 weeks after injury, rats in the hyperbaric oxygen group showed significant improvements in all measures compared with those in the model group ($P < 0.05$), although scores remained lower than in the sham group for the duration of the observation period ($P < 0.05$; **Figure 1**).

### Hyperbaric oxygen therapy reduced apoptosis in spinal cord tissue of rats with spinal cord injury

In the model group, TUNEL-positive cells were scattered throughout the injured spinal cord tissue and at the edge of the injury site. In the group that received hyperbaric oxygen therapy, however, significantly fewer apoptotic cells were observed than in the model group ($P < 0.05$). No apoptotic cells were observed in the sham group (**Figure 2**).

### Hyperbaric oxygen therapy reduced AQP4/9 mRNA and protein expression in spinal cord of rats with spinal cord injury

Reverse transcription PCR and western blot analysis revealed that AQP4/9 mRNA and protein expression levels were significantly greater in the model group than in the sham group 72 hours after spinal cord injury ($P < 0.05$). However, this elevated expression was attenuated in the hyperbaric oxygen therapy group ($P < 0.05$; **Figure 3**).

### Hyperbaric oxygen therapy improved pathological changes in spinal cord of rats with spinal cord injury

Hematoxylin-eosin staining showed that spinal cord tissue structure was intact and clear 4 weeks after injury, with no syringomyelia or neuronal apoptosis in the sham-operated rats. In the model group, spinal cord structure was loose and syringomyelia was observed, with a large number of necrotic neurons. In the hyperbaric oxygen therapy group, spinal cord structure was loose, with smaller cavities and fewer necrotic neurons than in the model group (**Figure 4**). Immunohistochemical staining revealed densely arranged NF-200-positive nerve fibers in the spinal cord of rats from the sham group. In comparison, there were fewer NF-200-positive nerve fibers in the spinal cord of rats in the model group ($P < 0.05$), and nerve fibers were short and sparsely arranged. After hyperbaric oxygen therapy, the number of NF-200-positive nerve fibers was greater than that in the model group ($P < 0.05$; **Figure 4**).

### Hyperbaric oxygen therapy improved neurological function in rats with spinal cord injury

Four weeks after spinal cord injury, hindlimb evoked potential waveforms were completely absent in the model and hyperbaric oxygen groups (data not shown). Four weeks after spinal cord injury, somatosensory evoked potentials and motor evoked potentials had recovered to a greater extent in the hyperbaric oxygen group than in the model group ($P < 0.05$; **Figure 5**).

## Discussion

Previous studies have shown that excessive inflammation promoted oligodendrocyte apoptosis, aggravated spinal cord injury, and hindered recovery of neurological function after spinal cord injury (Pallini et al., 2005; Pearse et al., 2007). In the early stages after acute spinal cord injury, disruption of microcirculation may trigger local hypoxia and ischemia, and cause immune inflammation. During this period, tumor necrosis factor-α, interleukin-1 and other inflammatory factors are released, and activation, proliferation and migration of microglia and astrocytes occurs, contributing to secondary cytotoxicity and scar formation. Sustained spinal cord ischemia/hypoxia and metabolic disorders are not conducive to neuronal and axonal regeneration, resulting in further secondary spinal cord injury (Crowe et al., 1997; Liu et al., 1997; Amar and Levy, 1999; Kwon et al., 2004; Banno et al.,

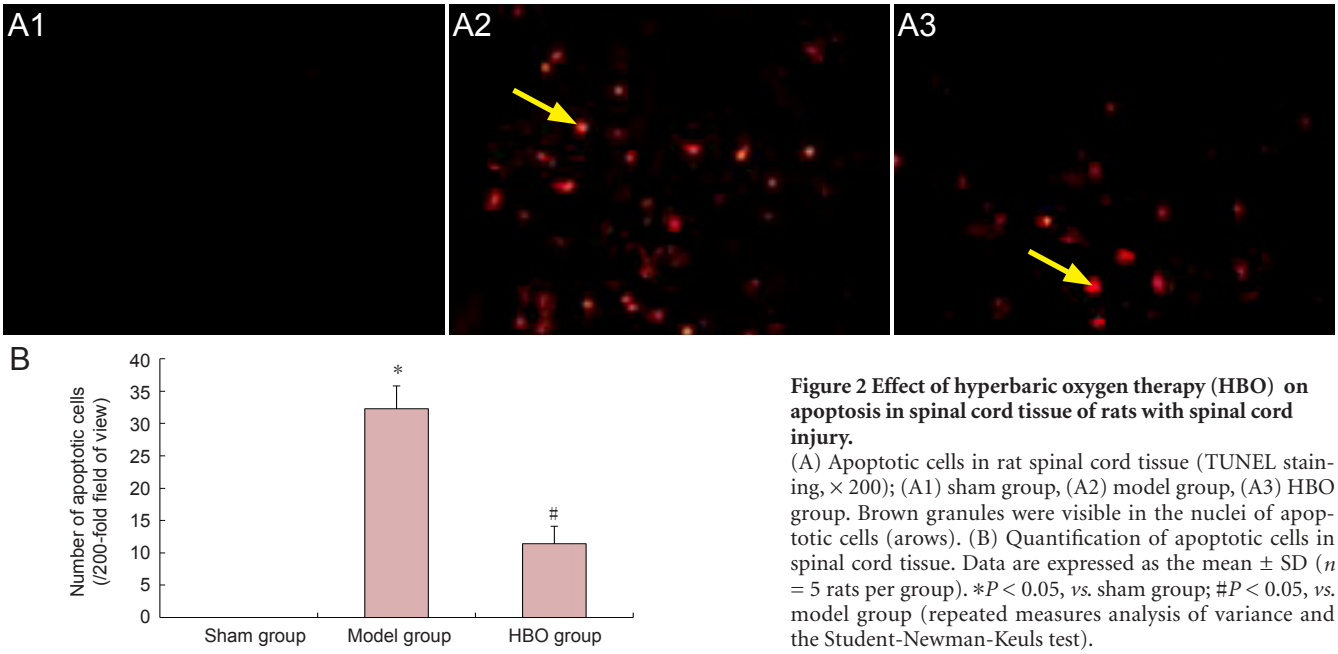


**Figure 2 Effect of hyperbaric oxygen therapy (HBO) on apoptosis in spinal cord tissue of rats with spinal cord injury.**

(A) Apoptotic cells in rat spinal cord tissue (TUNEL staining, × 200); (A1) sham group, (A2) model group, (A3) HBO group. Brown granules were visible in the nuclei of apoptotic cells (arows). (B) Quantification of apoptotic cells in spinal cord tissue. Data are expressed as the mean ± SD ($n$ = 5 rats per group). *$P$ < 0.05, *vs.* sham group; #$P$ < 0.05, *vs.* model group (repeated measures analysis of variance and the Student-Newman-Keuls test).

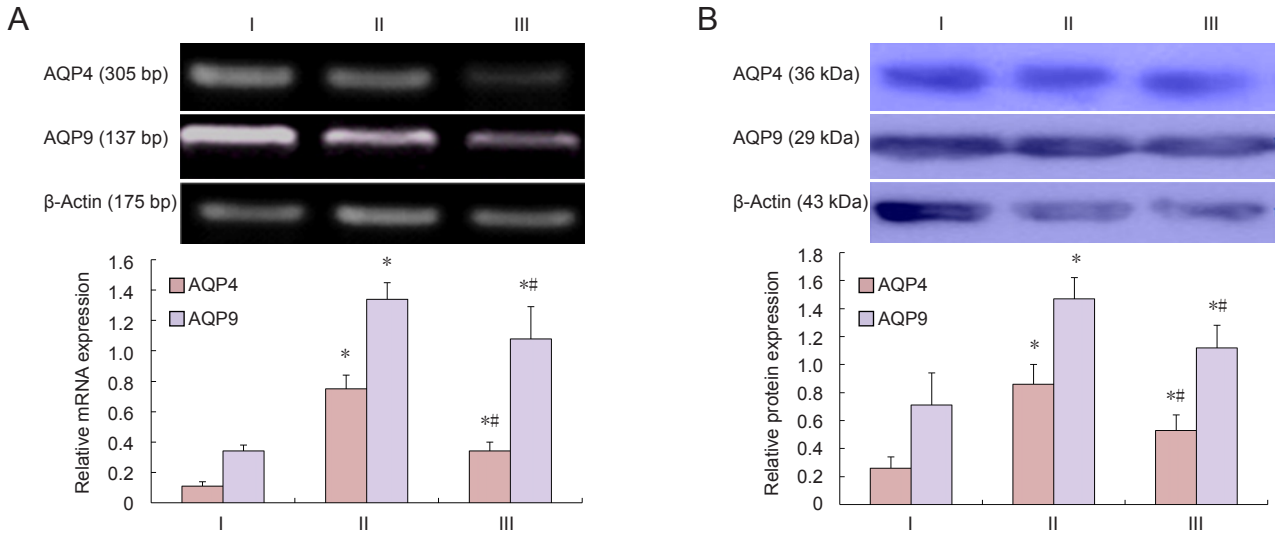


**Figure 3 Effect of hyperbaric oxygen therapy on aquaporin (AQP) 4/9 mRNA (A) and protein (B) expression levels in spinal cord of rats with spinal cord injury.**

(A) The integrated optical density ratio of the target gene to β-actin was calculated for each mRNA sample. (B) The integrated optical density ratio of the target protein to β-actin was calculated for each protein sample. Data are expressed as the mean ± SD ($n$ = 9 rats per group). *$P$ < 0.05, *vs.* sham group; #$P$ < 0.05, *vs.* model group (repeated measures analysis of variance and the Student-Newman-Keuls test). I: Model group; II: hyperbaric oxygen therapy group; III: sham group.

2005; Ohta et al., 2005). In the present study, we have shown that hyperbaric oxygen therapy administered immediately after spinal cord injury promotes recovery in rats by reducing the expression of edema-related genes and proteins in the injured spinal cord, attenuating apoptosis at the injury site, shortening the latency and increasing the amplitude of evoked potentials, and improving hindlimb motor function.

We propose the following mechanisms for the action of hyperbaric oxygen therapy in improving the microenvironment in the injured spinal cord: (1) Spinal cord injury causes local edema and hypoxia, and hyperbaric oxygen therapy reduces hypoxia-induced neuronal apoptosis by elevating the blood oxygen concentration in the injured spinal cord. (2) Hyperbaric oxygen downregulates AQP4/9 gene and protein expression, attenuating inflammation in the injured spinal cord. (3) The treatment also corrects acidosis in the injured spinal cord, improves the microcirculation, contributes to the maintenance of energy metabolism, and promotes the

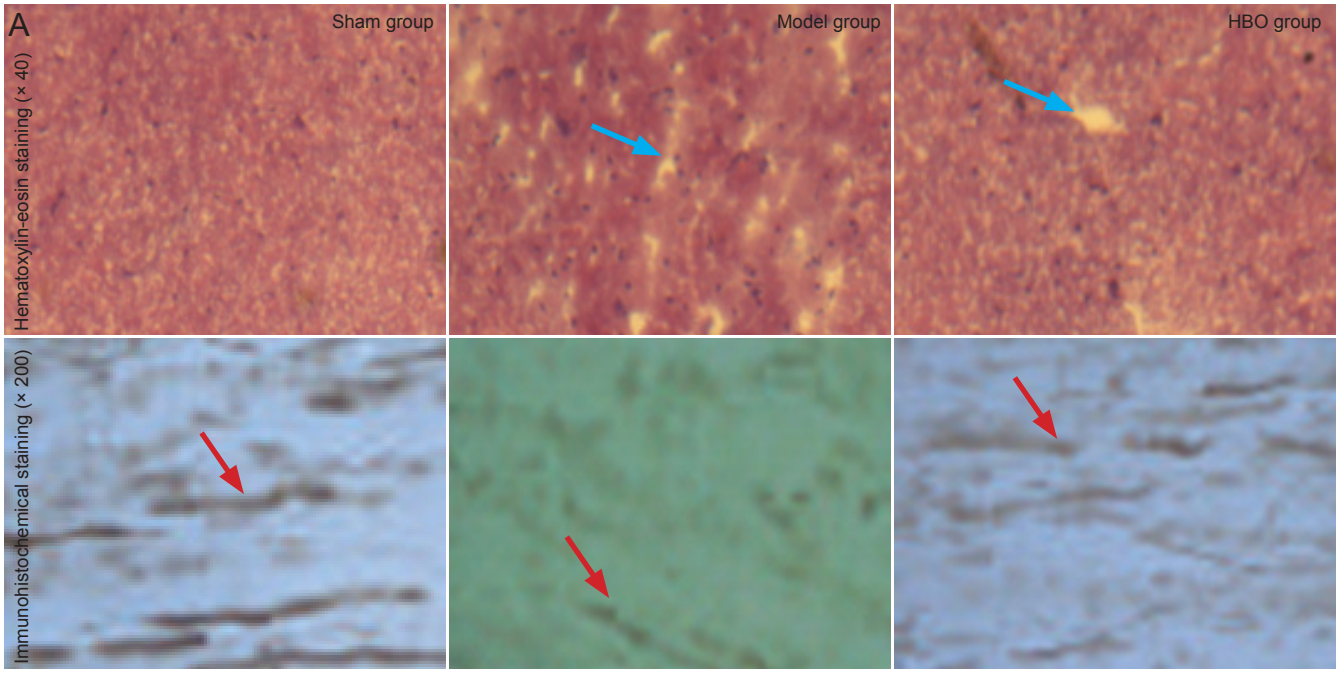


**Figure 4 Effect of hyperbaric oxygen therapy (HBO) on NF-200-positive nerve fibers in the spinal cord of rats with spinal cord injury.**
(A) Effect of hyperbaric oxygen therapy on pathological change of spinal cord. Syringomyelia (blue arrows) and loss of NF-200-positive fibers (red arrows) were attenuated after hyperbaric oxygen therapy. (B) Quantification of NF-200-positive nerve fibers in the spinal cord. Hyperbaric oxygen therapy reduced NF-200-positive fiber loss after spinal cord injury. Data are expressed as the mean ± SD ($n$ = 5 rats per group). *$P$ < 0.05, *vs.* sham group; #$P$ < 0.05, *vs.* model group (repeated measures analysis of variance and the Student-Newman-Keuls test).

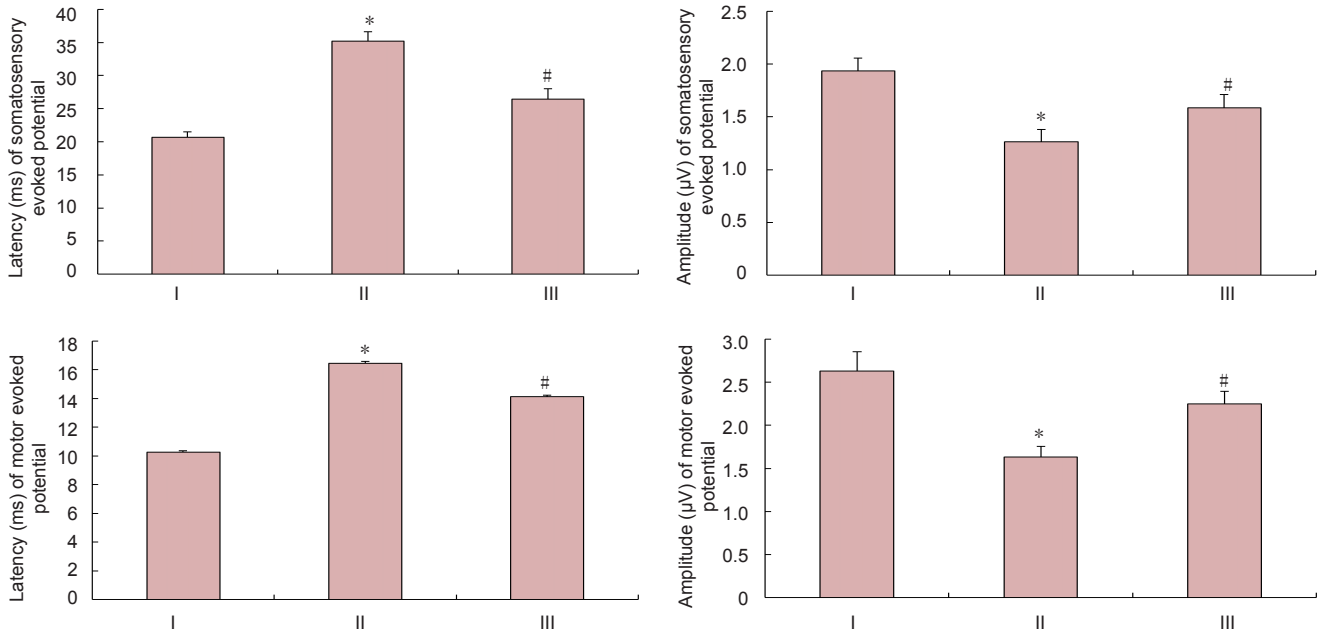


**Figure 5 Effect of hyperbaric oxygen therapy (HBO) on neurological function in rats with spinal cord injury.**
Data are expressed as the mean ± SD ($n$ = 7 rats per group). *$P$ < 0.05, *vs.* sham group; #$P$ < 0.05, *vs.* model group (repeated measures analysis of variance and the Student-Newman-Keuls test). I: Model group; II: HBO group; III: sham group.

recovery of neuronal function after reversible injury.

In summary, hyperbaric oxygen therapy helps to reduce neuronal apoptosis, lower the degree of disability, and prevent deterioration after spinal cord injury. The long-term efficacy, safety and reliability of this treatment, and minimal associated complications, make hyperbaric oxygen therapy a promising new treatment for spinal cord injury.

**Author contributions:** *Wang Y provided and integrated experimental data. Zhang SQ and Luo M were responsible for the study concept and design, and analyzing experimental data. Wang Y drafted the manuscript, supervised the study, performed statistical analysis, and was the head of the funds. Li YJ provided technical or information support, and instructed the experiments. All authors approved the final version of the manuscript.*

**Conflicts of interest:** *None declared.*

## References

Albin RL, Mink JW (2006) Recent advances in Tourette syndrome research. Trends Neurosci 29:175-182.

Amar AP, Levy ML (1999) Pathogenesis and pharmacological strategies for mitigating secondary damage in acute spinal cord injury. Neurosurgery 44:1027-1039.

Ariake K, Ohtsuka H, Motoi F, Douchi D, Oikawa M, Rikiyama T, Fukase K, Katayose Y, Egawa S, Unno M (2012) GCF2/LRRFIP1 promotes colorectal cancer metastasis and liver invasion through integrin-dependent RhoA activation. Cancer Lett 325:99-107.

Banno M, Mizuno T, Kato H, Zhang G, Kawanokuchi J, Wang J, Kuno R, Jin S, Takeuchi H, Suzumura A (2005) The radical scavenger edaravone prevents oxidative neurotoxicity induced by peroxynitrite and activated microglia. Neuropharmacology 48:283-290.

Block F, Schwarz M, Sontag KH (1993) Non-NMDA-mediated transmission of somatosensory-evoked potentials in the rat thalamus. Brain Res Bull 31:449-454.

Chang DJ, Jeong MY, Song J, Jin CY, Suh YG, Kim HJ, Min KH (2011) Discovery of small molecules that enhance astrocyte differentiation in rat fetal neural stem cells. Bioorg Med Chem Lett 21:7050-7053.

Chuang SK (2011) Limited evidence to demonstrate that the use of hyperbaric oxygen (HBO) therapy reduces the incidence of osteoradionecrosis in irradiated patients requiring tooth extraction. J Evid Based Dent Pract 11:129-131.

Crowe MJ, Bresnahan JC, Shuman SL, Masters JN, Beattie MS (1997) Apoptosis and delayed degeneration after spinal cord injury in rats and monkeys. Nat Med 3:73-76.

Ding JD (2012) Effect of hyperbaric oxygen therapy on serum ACA level in patients with acute cerebral infarction. Zhongguo Shiyong Shenjing Jibing Zazhi 15:34-36.

Fenton LH, Robinson MB (1993) Repeated exposure to hyperbaric oxygen sensitizes rats to oxygen-induced seizures. Brain Res 632:143-149.

Finch AM, Wong AK, Paczkowski NJ, Wadi SK, Craik DJ, Fairlie DP, Taylor SM (1999) Low-molecular-weight peptidic and cyclic antagonists of the receptor for the complement factor C5a. J Med Chem 42: 1965-1974.

Gomez-Iturriaga A, Crook J, Evans W, Saibishkumar EP, Jezioranski J (2011) The efficacy of hyperbaric oxygen therapy in the treatment of medically refractory soft tissue necrosis after penile brachytherapy. Brachytherapy 10:491-497.

Guo BF, Dong MM (2009) Application of neural stem cells in tissue-engineered artificial nerve. Otolaryngol Head Neck Surg 140:159-164.

Guo J, Wang J, Liang C, Yan J, Wang Y, Liu G, Jiang Z, Zhang L, Wang X, Wang Y, Zhou X, Liao H (2013) proNGF inhibits proliferation and oligodendrogenesis of postnatal hippocampal neural stem/progenitor cells through p75NTR in vitro. Stem Cell Res 11:874-887.

Jiao Q, Xie WL, Wang YY, Chen XL, Yang PB, Zhang PB, Tan J, Lu HX, Liu Y (2013) Spatial relationship between NSCs/NPCs and microvessels in rat brain along prenatal and postnatal development. Int J Dev Neurosci 31:280-285.

Kunke D, Bryja V, Mygland L, Arenas E, Krauss S (2009) Inhibition of canonical Wnt signaling promotes gliogenesis in P0-NSCs. Biochem Biophys Res Commun 386:628-633.

Kwon BK, Tetzlaff W, Grauer JN, Beiner J, Vaccaro AR (2004) Pathophysiology and pharmacologic treatment of acute spinal cord injury. Spine J 4:451-464.

Liu XZ, Xu XM, Hu R, Du C, Zhang SX, McDonald JW, Dong HX, Wu YJ, Fan GS, Jacquin MF, Hsu CY, Choi DW (1997) Neuronal and glial apoptosis after traumatic spinal cord injury. J Neurosci 17:5395-5406.

Liu YY, Yin HY, Cui WB, Zhu MZ, Chu LH, Yu CY (2004) Study of long-term effectiveness of the hyperbaric oxygen therapy in neonatal hypoxic-ischemic encephalopathy. Zhonghua Hanghai Yixue yu Gaoqiya Yixue Zazhi 11:87-90.

Meletis K, Barnabé-Heider F, Carlén M, Evergren E, Tomilin N, Shupliakov O, Frisén J (2008) Spinal cord injury reveals multilineage differentiation of ependymal cells. PLoS Biol 6:e182.

Mukai M, Savard PY, Ouellet H, Guertin M, Yeh SR (2002) Unique ligand-protein interactions in a new truncated hemoglobin from mycobacterium tuberculosis. Biochemistry 41:3897-3905.

Ohta S, Iwashita Y, Takada H, Kuno S, Nakamura T (2005) Neuroprotection and enhanced recovery with edaravone after acute spinal cord injury in rats. Spine 30:1154-1158.

Pallini R, Vitiani LR, Bez A, Casalbore P, Facchiano F, Di Giorgi Gerevini V, Falchetti ML, Fernandez E, Maira G, Peschle C, Parati E (2005) Homologous transplantation of neural stem cells to the injured spinal cord of mice. Neurosurgery 57:1014-1025.

Papastefanaki F, Chen J, Lavdas AA, Thomaidou D, Schachner M, Matsas R (2007) Grafts of Schwann cells engineered to express PSA-NCAM promote functional recovery after spinal cord injury. Brain 130:2159-2174.

Paxinos G, Watson C (2005) The Rat Brain in Stereotaxic Coordinates. London: Academic Press.

Pearse DD, Sanchez AR, Pereira FC, Andrade CM, Puzis R, Pressman Y, Golden K, Kitay BM, Blits B, Wood PM, Bunge MB (2007) Transplantation of Schwann cells and/or olfactory ensheathing glia into the contused spinal cord: survival, migration, axon association, and functional recovery. Glia 55:976-1000.

Tong L, Ji L, Wang Z, Tong X, Zhang L, Sun X (2010) Differentiation of neural stem cells into Schwann-like cells in vitro. Biochem Biophys Res Commun 401:592-597.

Xiong Z, Zhao S, Mao X, Lu X, He G, Yang G, Chen M, Ishaq M, Ostrikov K (2014) Selective neuronal differentiation of neural stem cells induced by nanosecond microplasma agitation. Stem Cell Res 12:387-399.

Young W (2002) Spinal cord contusion models. Prog Brain Res 137: 231-255.

Yu M, Jiang M, Yang C, Wu Y, Liu Y, Cui Y, Huang G (2014) Maternal high-fat diet affects Msi/Notch/Hes signaling in neural stem cells of offspring mice. J Nutr Biochem 25:227-231.

*Copyedited by Murphy JS, Norman C, Yu J, Yang Y, Li CH, Song LP, Zhao M*